

Novel organosoluble fluorinated polyimides derived from 1,6-bis(4-amino-2-trifluoromethylphenoxy)naphthalene and aromatic dianhydrides

Cheng-Lin Chung, Sheng-Huei Hsiao*

Department of Chemical Engineering, Tatung University, Taipei 104, Taiwan

ARTICLE INFO

Article history:

Received 2 February 2008

Received in revised form 5 March 2008

Accepted 24 March 2008

Available online 8 April 2008

Keywords:

Fluorinated polyimides

Optical transparency

Low dielectric constants

ABSTRACT

A novel trifluoromethyl-substituted bis(ether amine) monomer, 1,6-bis(4-amino-2-trifluoromethylphenoxy)naphthalene, was prepared through the nucleophilic substitution reaction of 2-chloro-5-nitrobenzotrifluoride and 1,6-dihydroxynaphthalene in the presence of potassium carbonate in dimethyl sulfoxide, followed by catalytic reduction with hydrazine and Pd/C in ethanol. A series of new fluorinated polyimides were synthesized from the diamine with various commercially available aromatic tetracarboxylic dianhydrides via a conventional two-stage process with the thermal or chemical imidization of the poly(amic acid) precursors. Most of the polyimides obtained from both routes were soluble in many organic solvents such as *N*-methyl-2-pyrrolidone and *N,N*-dimethylacetamide. All the polyimides could afford transparent, flexible, and strong films with low moisture absorptions of 0.12–0.52% and low dielectric constants of 2.75–3.13 at 10 kHz. Thin films of these polyimides showed an UV–vis absorption cutoff wavelength at 376–428 nm, and those of polyimides from 4,4'-oxydiphthalic dianhydride (ODPA) and 2,2-bis(3,4-dicarboxyphenyl)hexafluoropropane dianhydride (6FDA) were essentially colorless. The polyimides exhibited excellent thermal stability, with decomposition temperatures (at 10% weight loss) above 530 °C in both air and nitrogen atmospheres and glass transition temperatures (T_g s) in the range of 241–298 °C. For a comparative study, some properties of the present fluorinated polyimides were compared with those of structurally related ones prepared from 1,6-bis(4-aminophenoxy)naphthalene and 2,6-bis(4-amino-2-trifluoromethylphenoxy)naphthalene.

© 2008 Elsevier Ltd. All rights reserved.

1. Introduction

Aromatic polyimides possess many useful properties, such as high glass transition temperature, excellent dimensional stability, low dielectric constants and outstanding thermal and thermo-oxidative stabilities; therefore, they are widely used as an interlayer dielectrics, flexible circuitry substrates, stress buffers, and passivation layers [1]. Despite their widespread use, most of them have high melting or softening temperatures and limited solubility in most organic solvents because of their rigid backbones and strong intermolecular interactions, which may restrict their applications in some fields. For such difficulties to be overcome, polymer structure modification becomes necessary. Considerable research efforts have been achieved in designing and synthesizing new dianhydrides [2–14] and/or diamines [15–24]; thus, producing a great variety of soluble and processable polyimides for various purposes. The common strategies that enhance the tractability of polyimides include introduction of flexible linkages, bulky

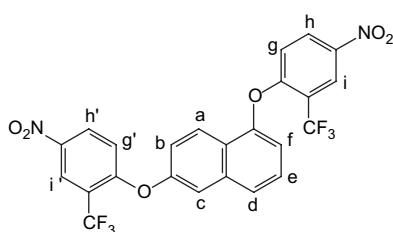
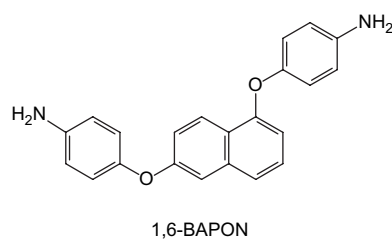
substituents, non-coplanar or alicyclic structures, and structurally unsymmetrical segments into the polymer backbone. The main concept behind these approaches is the reduction of intermolecular interactions, such as chain packing, charge-transfer complexing, and electronic polarization interactions.

Furthermore, a low dielectric constant is one of the most attractive properties of polyimide materials for microelectronics applications. In order to achieve a polymer structure with a low dielectric constant, repeating units with low polarity and low polarizability have to be used [25]. For example, the incorporation of aliphatic adamantane or diamantane moiety is known to result in low dielectric constants because of high hydrophobicity, low polarity, and increased free volume [26–29]. Another efficient method to reduce dielectric constants of polyimides is to introduce fluorine (F) groups into polyimide backbones because of the low electronic polarizability of the C–F bond as well as the increase of fractional free volume [30–34]. In recent years, polyimides containing pendent trifluoromethyl (CF₃) groups are of special interest [35–47]. An additional positive effect of fluorinated substituents is to enhance the solubility and optical transparency of polyimides. In view of the fact that polyimides derived from ether-bridged aromatic diamines with CF₃ group are generally soluble high

* Corresponding author.

E-mail address: shhsiao@ttu.edu.tw (S.-H. Hsiao).

temperature polymer materials with low moisture uptake, low dielectric constant, and high optical transparency, the present study reports the synthesis of a new CF₃-substituted bis(ether amine), 1,6-bis(4-amino-2-trifluoromethylphenoxy)naphthalene, and its derived fluorinated polyimides by reacting the diamine with various aromatic tetracarboxylic dianhydrides. The polymers were subjected to the solubility tests, thermal, optical and dielectric property measurements and were compared to analogous counterparts prepared from a non-fluorinated bis(ether amine), 1,6-bis(4-aminophenoxy)naphthalene (1,6-BAPON) [48]. The fluorine-containing polyimides were expected to exhibit enhanced solubility and diminished dielectric constants because of the increased free volume and hydrophobicity caused by the CF₃ substituents. The solubility and thermal properties of obtained fluorine-containing polyimides will also be compared with those of structurally related ones derived from 2,6-bis(4-amino-2-trifluoromethylphenoxy)naphthalene that have been reported previously [40].



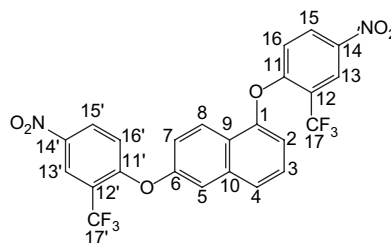
was purified by distillation under reduced pressure over calcium hydride and stored over 4 Å molecular sieves.

2.2. Monomer synthesis

2.2.1. 1,6-Bis(2-trifluoromethyl-4-nitrophenoxy)naphthalene (1)

1,6-Dihydroxynaphthalene (8.0 g, 0.05 mol) and 2-chloro-5-nitrobenzotrifluoride (23.0 g, 0.10 mol) were dissolved in 80 mL of dimethyl sulfoxide (DMSO) in a 300-mL round-bottomed flask. Then, potassium carbonate (14.0 g, 0.10 mol) was added, and the solution was heated at 120 °C for 24 h. The mixture was allowed to cool and then poured into 800 mL of water to give a yellow solid, which was collected, washed repeatedly with water, and dried. The crude product was recrystallized from methanol/water to give pale-yellow crystals (21.8 g, 81%); mp = 108–110 °C (onset to peak top temperature), by differential scanning calorimetry (DSC) at a scan rate of 2 °C/min.

IR (KBr): 1527, 1351 (–NO₂), 1270 (C–O stretch), 1141 cm^{–1} (C–F stretch). ¹H NMR (CDCl₃, δ, ppm): 8.61, 8.65 [d, J = 2.5 Hz, 2H, H_i and H_{i'}], 8.29, 8.32 [dd, J = 9.1, 2.5 Hz, 2H, H_h and H_{h'}], 8.06 (d, J = 9.1 Hz, 1H, H_d), 7.80 (d, J = 8.3 Hz, 1H, H_a), 7.66 (d, J = 2.1 Hz, 2H, H_c), 7.61 (t, J = 7.9 Hz, 1H, H_e), 7.32 (dd, J = 9.1, 2.2 Hz, 1H, H_b), 7.26 (d, J = 7.3 Hz, 1H, H_f), 6.90, 7.04 [dd, J = 9.1 Hz, 2H, H_g and H_{g'}]. ¹³C NMR (CDCl₃, δ, ppm): 160.7 (C^{11'}), 160.2 (C¹¹), 152.9 (C⁶), 149.5 (C¹), 142.2 (C^{14'}), 142.1 (C¹⁴), 133.0 (C¹⁰), 131.4 (C⁸), 128.9 (C^{15'}), 128.7 (C¹⁵), 127.4 (C⁹), 126.2 (C⁴), 126.0 (C³), 123.9 [m, ³J_{C–F} = 5 Hz, C¹³ and C^{13'}], 121.1 (q, ¹J_{C–F} = 271 Hz, C^{17'}), 121.2 (C⁷), 121.2 (q, ²J_{C–F} = 30 Hz, C^{12'}), 120.9 (q, ¹J_{C–F} = 271 Hz, C¹⁷), 120.8 (q, ²J_{C–F} = 30 Hz, C¹²), 117.8 (C^{16'}), 117.6 (C²), 116.7 (C¹⁶), 111.0 (C⁵). Anal. Calcd. for C₂₄H₁₂F₆N₂O₆ (538.36): C, 53.54%; H, 2.24%; N, 5.20%. Found: C, 53.51%; H, 2.15%; N, 4.81%.



2. Experimental

2.1. Materials

1,6-Dihydroxynaphthalene (Tokyo Chemical Industry; TCI), potassium carbonate (K₂CO₃) (Fluka), 2-chloro-5-nitrobenzotrifluoride (Acros), *p*-chloronitrobenzene (Acros), 10% palladium on charcoal (Pd/C) (Fluka), and hydrazine monohydrate (Acros) were used as-received. As reported in a previous paper [49], 1,6-BAPON (mp = 163–164 °C) was prepared by the nucleophilic aromatic substitution reaction of 1,6-dihydroxynaphthalene with *p*-chloronitrobenzene in the presence of K₂CO₃ and the subsequent reduction of the intermediate dinitro compound with hydrazine as the reducing agent and palladium as the catalyst. Commercially available aromatic tetracarboxylic dianhydrides such as pyromellitic dianhydride (PMDA) (**3a**) (Aldrich) and 3,3',4,4'-benzophenonetetracarboxylic dianhydride (BTDA) (**3c**) (Aldrich) were purified by recrystallization from acetic anhydride. 3,3',4,4'-Biphenyltetracarboxylic dianhydride (BPDA) (**3b**) (Oxychem), 3,3',4,4'-diphenylsulfonetetracarboxylic dianhydride (DSDA) (**3d**) (New Japan Chemical Co.), and 4,4'-oxydiphthalic dianhydride (ODPA) (**3e**) (Oxychem) and 2,2-bis(3,4-dicarboxyphenyl)hexafluoropropane dianhydride (6FDA) (**3f**) (Hoechst Celanese) were heated at 250 °C under vacuum for 3 h prior to use. *N,N*-Dimethylacetamide (DMAc)

2.2.2. 1,6-Bis(4-amino-2-trifluoromethylphenoxy)naphthalene (2)

A mixture of the purified dinitro compound **1** (20.1 g, 0.037 mol), 10% Pd/C (0.15 g), ethanol (100 mL), and hydrazine monohydrate (10 mL) was heated at reflux temperature for about 8 h. The resulting clear, darkened solution was filtered hot to remove Pd/C, and the filtrate was then distilled to remove the solvent. The crude product was purified by recrystallization from acetone/water to give pale-yellow crystals (13.9 g, 78%); mp = 171–173 °C by DSC (2 °C/min).

IR (KBr): 3482, 3453, 3361 (N–H stretch), 1226 (C–O stretch), 1128 cm^{–1} (C–F stretch). ¹H NMR (CDCl₃, δ, ppm; for peak assignments: see Fig. 1(a)): 8.29 (d, J = 9.2 Hz, 1H, H_d), 7.38 (d, J = 8.3 Hz, 1H, H_a), 7.29 (t, J = 8.0 Hz, 1H, H_e), 7.27 (dd, J = 9.1, 2.5 Hz, 1H, H_b), 7.20 (d, J = 2.3 Hz, 1H, H_c), 7.01 [s, 2H (H_i, H_{i'})], 6.86, 6.95 [d, J = 8.7 Hz, 2H, H_g and H_{g'}], 6.77, 6.82 [dd, J = 8.7, 2.7 Hz, 2H, H_h and H_{h'}], 6.67 (d, J = 7.6 Hz, 1H, H_f), 3.72 (s, 4H, –NH₂). ¹³C NMR (CDCl₃, δ, ppm; for peak assignments: see Fig. 1(b)): 157.1 (C^{6'}), 154.2 (C¹), 146.1 (C^{11'}), 145.6 (C¹¹), 142.8 (C^{14'}), 142.5 (C¹⁴), 135.8 (C¹⁰), 126.6 (C³), 124.2 (C⁸), 123.2 (C^{16'}), 122.5 (C⁹), 122.2 (C¹⁶), 121.8 (C⁴), 119.3 (C^{15'}), 119.2 (C¹⁵), 118.9 (C⁷), 123.3 (q, ²J_{C–F} = 30 Hz, C^{12'}), 123.2 (q, ¹J_{C–F} = 271 Hz, C^{17'}), 123.1 (q, ¹J_{C–F} = 271 Hz, C¹⁷), 123.0 (q, ²J_{C–F} = 30 Hz, C¹²), 113.0 [m, ³J_{C–F} = 5 Hz, C¹³ and C^{13'}], 112.0 (C⁵), 107.7 (C^{2'}). Anal. Calcd. for C₂₄H₁₆F₆N₂O₂ (478.39): C, 60.26%; H, 3.37%; N, 5.85%. Found: C, 60.24%; H, 3.44%; N, 6.06%.

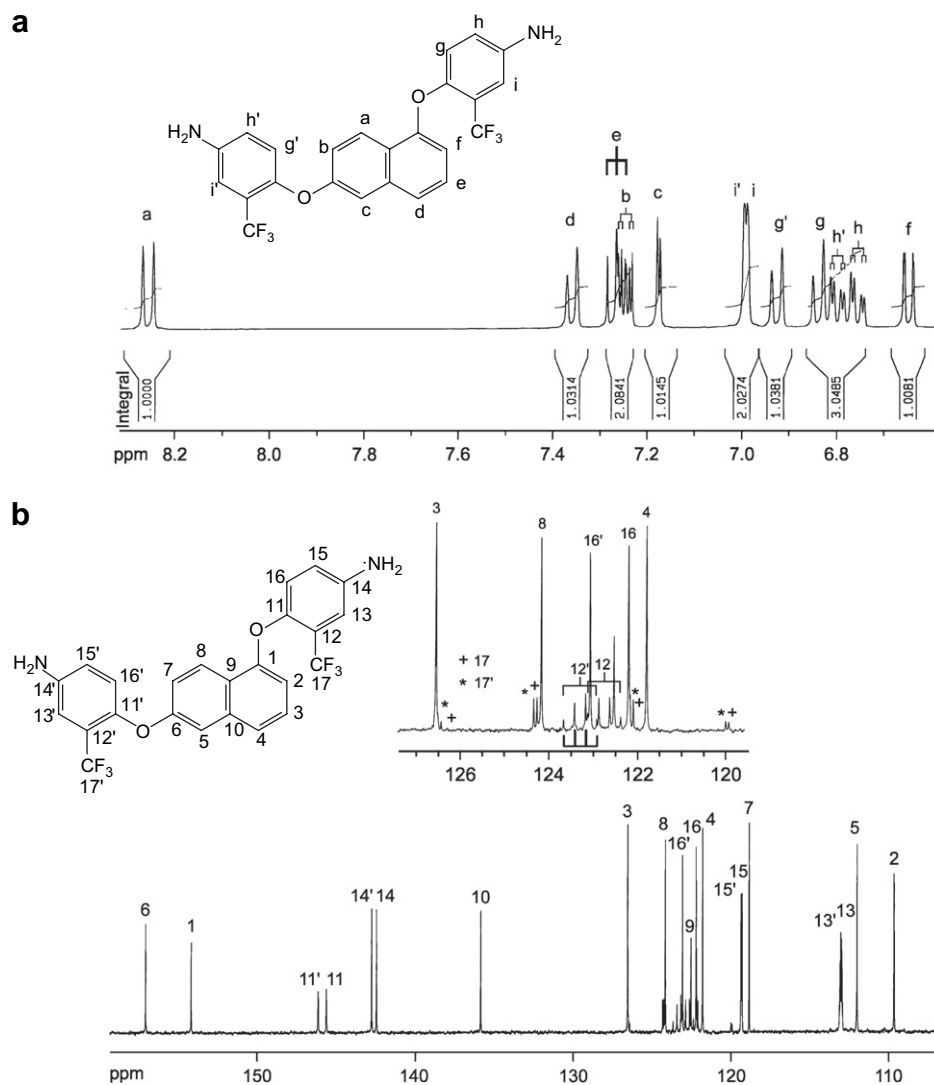


Fig. 1. (a) ¹H NMR and (b) ¹³C NMR spectra of CF₃-diamine **2** in CDCl₃. The accompanying amino group resonance (–NH₂; at 3.72 ppm) of **2** is not shown.

Crystal data: pale-yellow crystal grown during slow crystallization in acetone/water (1:2 v/v), 0.60 mm × 0.40 mm × 0.12 mm, orthorhombic *P*2₁2₁2₁ with *a* = 8.7630(2), *b* = 9.8520(3), *c* = 24.9440(8) Å, $\alpha = 90^\circ$, $\beta = 90^\circ$, and $\gamma = 90^\circ$, where *D*_c = 1.476 mg/m³ for *Z* = 4 and *V* = 2153.49(11) Å³.

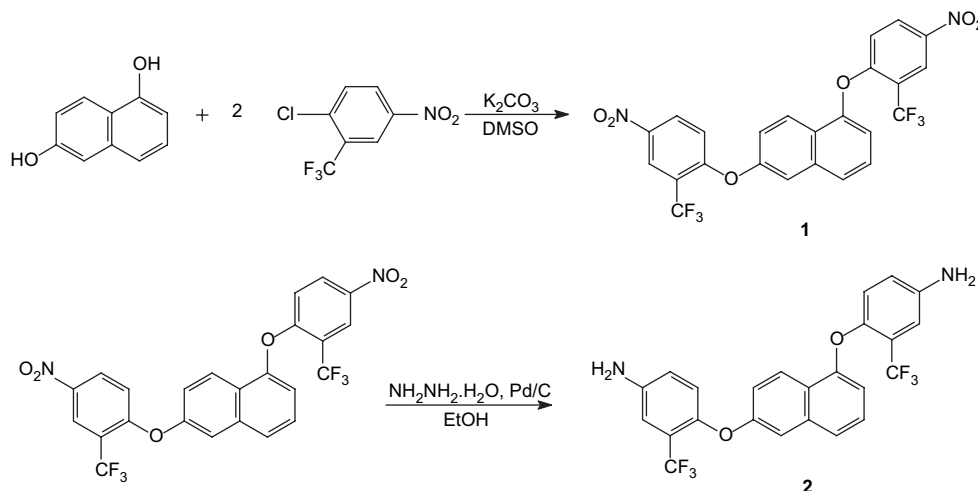
2.3. Polymer synthesis

The polyimides were synthesized from various dianhydrides and the diamine **2** via a conventional two-step method. The synthesis of polyimide **5f** is used as an example to illustrate the general synthetic route used to produce the polyimides. To a solution of 0.7778 g (1.62 mmol) of diamine **2** in 14.5 mL of CaH₂-dried DMAc in a 50-mL flask, 0.7222 g (1.62 mmol) of dianhydride 6FDA was added in one portion. Thus, the solid content of the solution is approximately 10 wt%. The mixture was stirred at room temperature overnight (for about 12 h) to afford a highly viscous poly(amic acid) solution. The inherent viscosity of the resulting poly(amic acid) **4f** was 1.07 dL/g, measured in DMAc at a concentration of 0.5 g/dL at 30 °C. The poly(amic acid) was subsequently converted to polyimide by either thermal or chemical imidization process. For the thermal imidization process, about 7 g of the obtained poly(amic acid) solution was poured into a 9-cm glass culture dish, which was placed overnight in a 90 °C oven to slowly release the

casting solvent. The semi-dried poly(amic acid) film was further dried and transformed into polyimide **5f** by sequential heating at 150 °C for 30 min, 200 °C for 30 min, and 250 °C for 1 h. The polyimide film was stripped from the glass substrate by being soaked in water. The inherent viscosity of the polyimide **5f** was 0.78 dL/g in DMAc at a concentration of 0.5 g/dL at 30 °C. For tensile test, dielectric and thermogravimetric analyses, the polyimide films were further heated at 300 °C for another 1 h. For the chemical imidization process, 5 mL of acetic anhydride and 2 mL of pyridine were added to the remaining poly(amic acid) solution, and the mixture was heated at 100 °C for 1 h to effect a complete imidization. The resulting polyimide solution was poured slowly into 250 mL of methanol giving rise to a fibrous precipitate, which was washed thoroughly with methanol and water, collected by filtration, and dried. The inherent viscosity of chemically imidized **5f** is 0.85 dL/g in DMAc, measured at a concentration of 0.5 g/dL at 30 °C. IR (film): 1785, 1727 (imide C=O stretch), 1379 (imide C–N stretch), 1259 (C–O stretch), 1141 cm^{−1} (C–F stretch).

2.4. Measurements

Elemental analyses were run in a PerkinElmer model 2400 C, H, N analyzer. Infrared spectra were recorded on a PerkinElmer spectrum GX FT-IR system. ¹H NMR and ¹³C NMR spectra were



Scheme 1. Synthesis of the diamine monomer 2.

measured on a JEOL EX 400 spectrometer with $CDCl_3$ as the solvent and tetramethylsilane as the internal reference. The inherent viscosities of the polymers were measured with an Ubbelohde viscometer at 30 °C. Weight-average molecular weights (M_w s) and number-average molecular weights (M_n s) were obtained via gel permeation chromatography (GPC) on the basis of polystyrene calibration using Waters 2410 as an apparatus and tetrahydrofuran (THF) as the eluent. Wide-angle X-ray diffraction (WAXD) measurements were performed at room temperature (about 25 °C) on a Shimadzu XRD 6000 X-ray diffractometer (40 kV, 20 mA), using graphite-monochromatized Cu-K α radiation. An Instron universal tester model 1130 with a load cell of 5 kg was used to study the stress–strain behavior of the polyimide film samples. A gauge length of 2 cm and a crosshead speed of 5 mm/min were used for this study. Measurements were performed at room temperature with film specimens (0.5 cm wide, 6 cm long, and about 0.09 mm thick), and an average of at least five individual determinations was used. The color intensity of the polymers was evaluated by a Gretag Macbeth Color-Eye 3100 colorimeter. Measurements were performed with films (83–93 μ m thick) with an observational angle 10° and a Commission International de l'Eclairage (CIE)-D illuminant. A CIE LAB color difference equation was used. Ultraviolet–visible (UV–vis) spectra of the polymer films were recorded on a Shimadzu UV–visible spectrophotometer UV-1601. Dielectric property of the polymer films was tested by the parallel-plate capacitor method using an HP-4194A Impedance/Gain Phase Analyzer. Gold electrodes were vacuum deposited on both surfaces of dried films. Experiments were performed at 25 °C in a dry chamber. Thermogravimetric analysis (TGA) was conducted with a Perkin-Elmer Pyris 1 TGA. Experiments were carried out on approximately 6–8 mg film samples heated in flowing nitrogen or air (flow rate 30 cm^3/min) at a heating rate of 20 °C/min. Differential scanning calorimetric (DSC) analyses were performed on a PerkinElmer Pyris 1 DSC at a scan rate of 20 °C/min in flowing nitrogen (20 cm^3/min). Glass transition temperatures (T_g s) were read at the middle of the transition in the heat capacity and were taken from the second heating scan after quick cooling from 400 °C at a cooling rate of 200 °C/min. Thermomechanical analysis (TMA) was conducted with a PerkinElmer TMA 7 instrument. The TMA experiments were conducted from 50 °C to 300 °C at a scan rate of 10 °C/min. A penetration probe of 1.0 mm in diameter and an applied constant load of 10 mN were used. Softening temperatures (T_s s) were taken as the onset temperature of probe displacement on the TMA traces. The equilibrium water absorption was determined by the weighing of the changes in vacuum-dried film specimens before and after immersion in deionized water at 25 °C for 3 days.

3. Results and discussion

3.1. Monomer synthesis

The new CF_3 -containing bis(ether amine) **2** was prepared in a two-step procedure as shown in Scheme 1. The first step is a Williamson etherification of 1,6-dihydroxynaphthalene with 2-chloro-5-nitrobenzotrifluoride in DMSO in the presence of potassium carbonate as a base. The diamine **2** was readily obtained in high yields by the catalytic reduction of intermediate dinitro compound **1** with hydrazine hydrate and Pd/C catalyst in refluxing ethanol. The structures of the dinitro compound **1** and the diamine monomer **2** were confirmed by elemental analysis as well as FTIR and NMR spectroscopic techniques. The nitro group of compound **1** gave two characteristic bands at 1596 cm^{-1} and 1351 cm^{-1} (NO_2 asymmetric and symmetric stretchings) in the IR spectrum. After reduction, the characteristic absorptions of the nitro group disappeared, and the amino group showed the typical N–H stretching bands in the region of 3300–3500 cm^{-1} . Fig. 1 illustrates the 1H NMR and ^{13}C NMR spectra of diamine monomer **2** in $CDCl_3$. Assignments of each carbon and proton are assisted by the two-dimensional NMR spectra shown in Figs. 2 and 3, and these spectra agree well with the proposed molecular structure of **2**. The 1H NMR spectrum confirms that the nitro groups have been completely converted into amino groups by the high field shift of the aromatic protons (especially for protons h, h', i, i') and by the signal at 3.72 ppm corresponding to the primary aromatic amine protons. In the ^{13}C NMR spectrum of diamine monomer **2**, almost all the carbon-13 atoms resonated in the region of 110–160 ppm, and there appeared six quartets because of the heteronuclear ^{13}C – ^{19}F coupling and its asymmetric structure. The large quartets centered at about 123.2 (C^{17}) ppm and 123.1 (C^{17}) ppm for **2** are peculiar to the CF_3 carbons. The one-bond C–F coupling constant in these cases is about 271 Hz. The CF_3 -attached carbons $C^{12'}$ and C^{12} also show clear quartets centered at 123.3 ppm and 123.0 ppm, respectively, with a small coupling constant of about 30 Hz due to two-bond C–F coupling. Besides, the $C^{13'}$ and C^{13} carbons (*ortho* to the CF_3 group) also have their resonances split by the three fluorines (three-bond coupling). The close multiplet (two overlapping quartets) had an even smaller coupling constant (ca. 5 Hz) because the interaction operated over more bonds. Therefore, all the spectroscopic data obtained are in good agreement with the expected structure of the target diamine monomer **2**. The molecular structure of **2** was also confirmed by X-ray crystal analysis. X-ray crystal data were acquired from the single crystal obtained by slow crystallization of an acetone/water solution. As shown in Fig. 4 the diamine monomer **2**

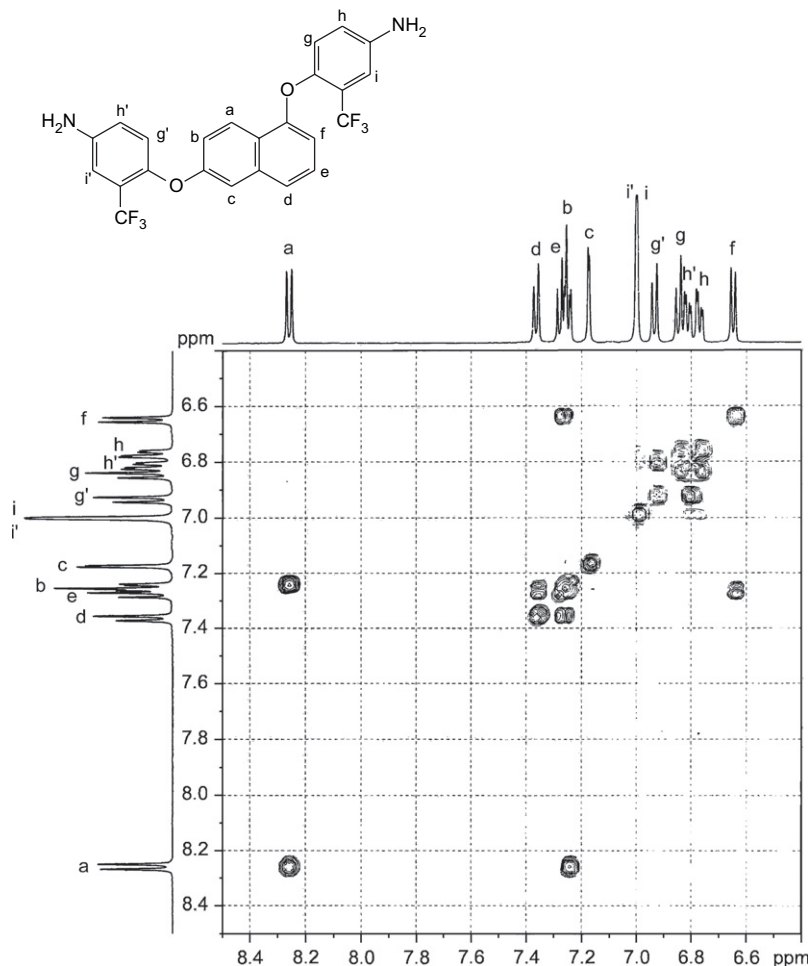


Fig. 2. H–H COSY spectrum of diamine monomer **2** in CDCl_3 .

displayed a highly distorted structure because of the unsymmetrical 1,6-catenated naphthalene unit and the bulky CF_3 group. Thus, the resulting polyimides from **2** should have a periodically twisted polymer backbone, and this would lower the chain packing and increase the solubility.

3.2. Polymer synthesis

The fluorinated polyimides **5a–5f** were prepared from diamine **2** and six commercially available dianhydrides **3a–3f** by a conventional two-step synthetic method as shown in Scheme 2. In spite of the presence of electron-withdrawing CF_3 substituents, the diamine **2** was still sufficiently reactive to give high molecular weight poly(amic acid)s when they were allowed to polymerize for a longer time (about 12 h). The diamine **2** mostly likely retained its reactivity because its amino group is *meta* to the CF_3 group. As shown in Table 1, the inherent viscosities of the intermediate poly(amic acid)s ranged from 0.94 dL/g to 1.21 dL/g. The molecular weights of all the poly(amic acid)s were sufficiently high to permit the casting of flexible and tough poly(amic acid) films, which were subsequently converted into tough polyimide films by extended heating at elevated temperatures. Some of the thermally cured polyimides exhibited excellent solubility in polar solvents such as NMP and DMAc. Therefore, the characterization of solution viscosity was carried out without any difficulty, and the inherent viscosities of the organosoluble polyimides were recorded in the range of 0.78–1.26 dL/g, as measured in DMAc at 30 °C. Table 1 also shows the molecular weights of **5d–5f** prepared by the thermal

imidization method. The weight-average molecular weights (M_w s) and number-average molecular weights (M_n s) were recorded in the ranges of 47,500–51,500 and 25,500–27,000, relative to polystyrene standards. The transformation from poly(amic acid) to a polyimide was also carried out via chemical cyclodehydration by using acetic anhydride and pyridine.

The chemical structures of the polyimides were characterized by IR and elemental analysis. Fig. 5 demonstrates a typical set of IR spectra for poly(amic acid) **4a** and polyimide **5a**. All the polyimides exhibited characteristic imide absorptions at around 1780 cm^{-1} and 1725 cm^{-1} (typical of imide carbonyl asymmetrical and symmetrical stretches), 1380 cm^{-1} (C–N stretch), and 1100 and 730 cm^{-1} (imide ring deformation), together with some strong absorption bands in the region of $1100\text{–}1300\text{ cm}^{-1}$ due to the C–O and C–F stretchings. The disappearance of amide and carboxyl bands indicates a virtually complete conversion of the poly(amic acid) precursor into polyimide. The results of the elemental analyses of all the thermally cured polyimides are listed in Table 2. The values found were in good agreement with the calculated ones of the proposed structures.

3.3. Properties of polyimides

The solubility of the polyimides was tested qualitatively in various organic solvents. The solubility properties of the thermally cured polyimides are reported in Table 3. All the fluorinated polyimides except **5a** and **5b** were soluble in strong dipolar solvents, such as NMP, DMAc, DMF, and DMSO, and phenol solvents like

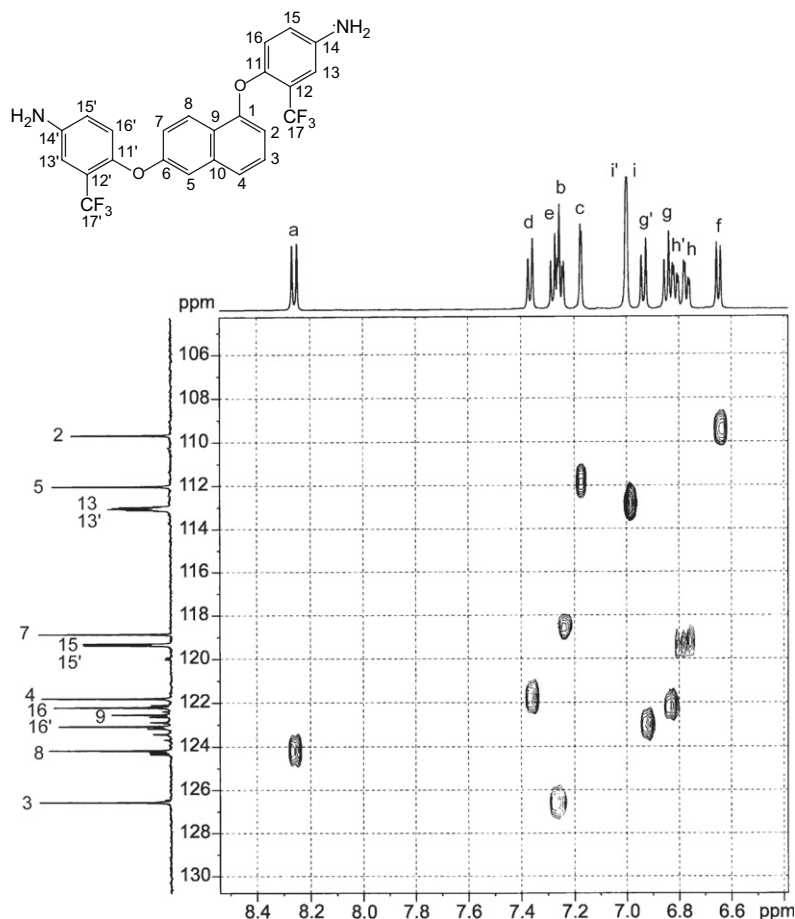


Fig. 3. C–H COSY spectrum of diamine monomer **2** in CDCl_3 .

m-cresol and 2-chlorophenol at room temperature or upon heating. The polyimides (**5c–5f**) derived from less stiff dianhydride components were also soluble in low boiling point organic solvents such as THF, 1,4-dioxane, and dichloromethane. Polyimides **5a** and **5b** showed a relatively lower solubility compared to the other polymers of the same series, which could be attributed to the more rigid nature of their backbones because of the rigid PMDA and BPDA components. For comparison, the solubility behavior of the corresponding analogues such as the 1,6-BAPON-derived, non-fluorinated **6** series and the fluorinated **7** series polyimides containing 2,6-naphthalenedioxy units reported previously [46,40] is also presented in Table 3. In general, the present fluorinated **5** series polyimides revealed an enhanced solubility than the respective **6** and **7** series ones, and this could be attributed to the molecular asymmetry and presence of bulky CF_3 groups in the former, which increased the disorder in the chains and hindered dense chain packing, thus, reducing the interchain interactions to enhance

solubility. The solubilities of the resulting polyimides **5a–5f** by chemical imidization were also investigated, and the result is presented in Table 4. The polyimide prepared by chemical imidization exhibited slightly high solubility than those by thermal curing. The less solubility of the latter is possibly due to the presence of partial interchain crosslinking during the thermal imidization process.

All of the fluorinated polyimides afforded good quality and creasable films with light color. These films were subjected to a tensile test, and their tensile properties are also reported in Table 1. The films exhibited ultimate tensile strengths of 107–133 MPa, elongations to break of 10–13%, and initial moduli of 2.03–2.28 GPa, indicating that they are strong and tough polymeric materials. The crystallinity of the polyimides was characterized by wide-angle X-ray diffraction (WAXD) studies. Two of the **6** series polyimides, **6a** and **6b**, displayed slightly semi-crystalline WAXD patterns, whereas all of the others showed amorphous patterns. In contrast to polyimides **6a** and **6b**, the corresponding fluorinated polyimides

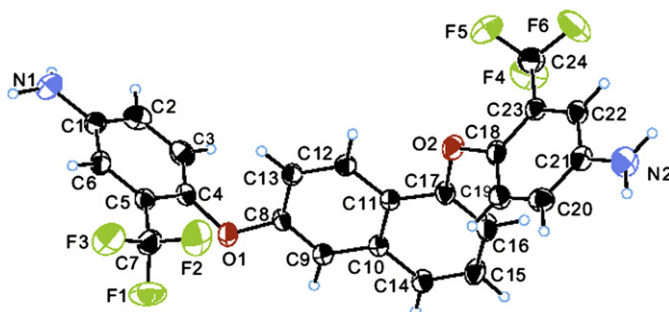


Fig. 4. X-ray crystal structure of diamine **2**.

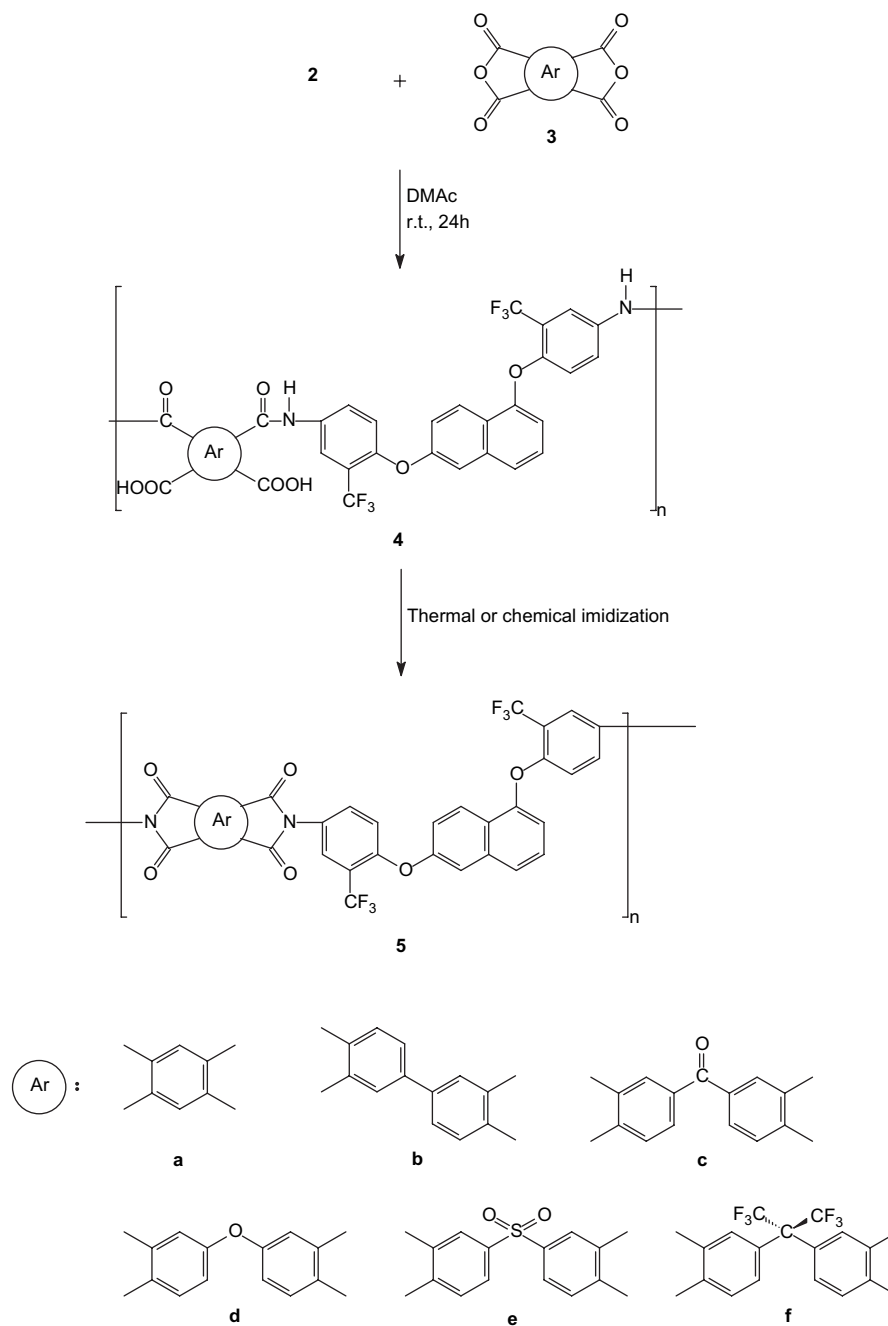


Table 1
Inherent viscosity of poly(amic acids) and polyimides and thin film tensile properties of the polyimides

Poly(amic acid)		Polyimide		GPC data of polyimides			Tensile properties of the polyimide films		
Code	η_{inh}^a (dL/g)	Code	η_{inh}^a (dL/g)	M_n	M_w	M_w/M_n	Tensile strength (MPa)	Elongation to break (%)	Initial modulus (GPa)
4a	0.94	5a	– ^b	– ^c			123	13	2.11
4b	0.98	5b	–				133	13	2.27
4c	1.07	5c	1.25				119	11	2.06
4d	1.13	5d	1.26	27,000	49,000	1.82	123	11	2.28
4e	1.21	5e	0.80	27,000	47,500	1.76	120	13	2.03
4f	1.07	5f	0.78	25,500	51,500	2.02	107	10	2.07

^a Measured at a polymer concentration of 0.5 g/dL in DMAc at 30 °C.

^b Insoluble in DMAc.

^c Insoluble in THF.

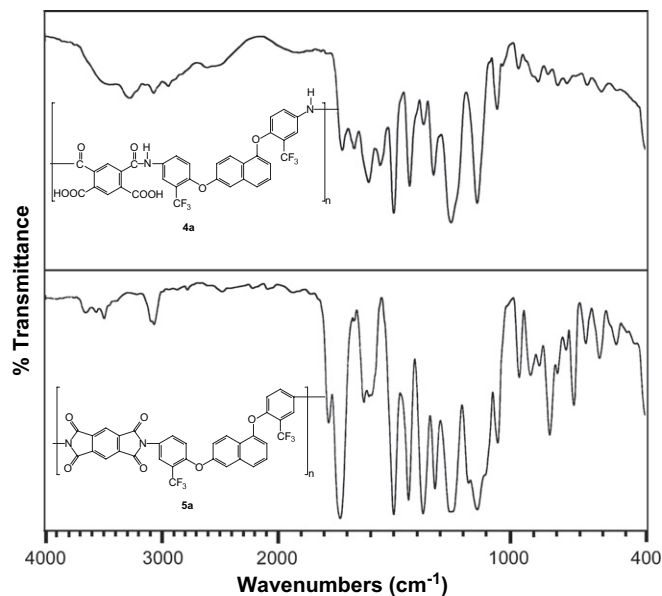


Fig. 5. IR spectra (film) of poly(amic acid) **4a** and polyimide **5a**.

5a and **5b** displayed nearly completely amorphous patterns. The amorphous nature of the fluorinated polyimides **5a–5f** is attributed not only to the bulkiness of the CF_3 substituent but also to the unsymmetrical structure coming from the diamine monomer.

Table 2
Elemental analysis of fluorinated polyimides prepared via thermal imidization

Polyimide	Formula of the repeat unit (formula weight)	C (%)		H (%)		N (%)	
		Calcd.	Found	Calcd.	Found	Calcd.	Found
5a	$\text{C}_{34}\text{H}_{14}\text{F}_6\text{N}_2\text{O}_6$ (660.49)	61.83	61.19	2.14	2.03	4.24	4.16
5b	$\text{C}_{40}\text{H}_{18}\text{F}_6\text{N}_2\text{O}_6$ (736.11)	65.23	64.56	2.46	2.56	3.80	3.84
5c	$\text{C}_{41}\text{H}_{18}\text{F}_6\text{N}_2\text{O}_7$ (764.10)	64.41	63.47	2.37	2.65	3.66	4.06
5d	$\text{C}_{40}\text{H}_{18}\text{F}_6\text{N}_2\text{O}_7$ (752.58)	63.84	63.71	2.41	2.38	3.72	3.67
5e	$\text{C}_{40}\text{H}_{18}\text{F}_6\text{N}_2\text{O}_8\text{S}$ (800.64)	60.00	59.19	2.27	2.42	3.50	3.40
5f	$\text{C}_{43}\text{H}_{18}\text{F}_{12}\text{N}_2\text{O}_6$ (886.61)	58.25	57.79	2.05	2.20	3.16	3.27

Table 3
Solubility behavior of the polyimides prepared via thermal imidization^a

Solvent ^b	Polyimide					
	5a	5b	5c	5d	5e	5f
NMP	+h (-/-) ^c	+h (-/+)	+h (-/+)	+(+h/+)	+(+h/+)	+(+h/+)
DMAc	+h (-/-)	+h (-/+h)	+ (-/-)	+(+h/+h)	+(+h/+h)	+(+h/+h)
DMF	+h (-/-)	- (-/-)	+h (-/+h)	+(+h/+h)	+(+h/+h)	+(+h/+h)
DMSO	- (-/-)	- (-/+)	+h (-/-)	+h (-/+h)	+h (+h/+h)	+(+h/+h)
<i>m</i> -Cresol	- (-/-)	+h (-/-)	+h (-/-)	+h (+h/-)	+h (-/-)	+h (+h/+h)
2-Chlorophenol	+h (-/-)	+h (-/-)	+h (-/-)	+h (+h/-)	+h (+h/-)	+(+h/+h)
THF	- (-/-)	- (-/-)	+h (-/-)	+ (-/-)	+ (-/-)	+(+h/+h)
1,4-Dioxane	- (-/-)	- (-/-)	+h (-/-)	+h (-/-)	+h (-/-)	+(+h/+h)
Dichloromethane	- (-/-)	- (-/-)	+h (-/-)	+ (-/-)	+ (-/-)	+(+h/+h)
Acetone	- (-/-)	- (-/-)	- (-/-)	- (-/-)	- (-/-)	+(+h/+h)

The symbol +: soluble at room temperature; +h: soluble on heating at 100 °C or boiling temperature; -: insoluble even on heating.

^a The solubility was determined by using 10 mg sample in 1 mL of stirred solvent.

^b NMP = *N*-methyl-2-pyrrolidone; DMAc = *N,N*-dimethylacetamide; DMF = *N,N*-dimethylformamide; DMSO = dimethyl sulfoxide; THF = tetrahydrofuran.

^c Data in parentheses are those for analogous polyimides (**6/7**) having the corresponding Ar units as in the **5** series polyimides.

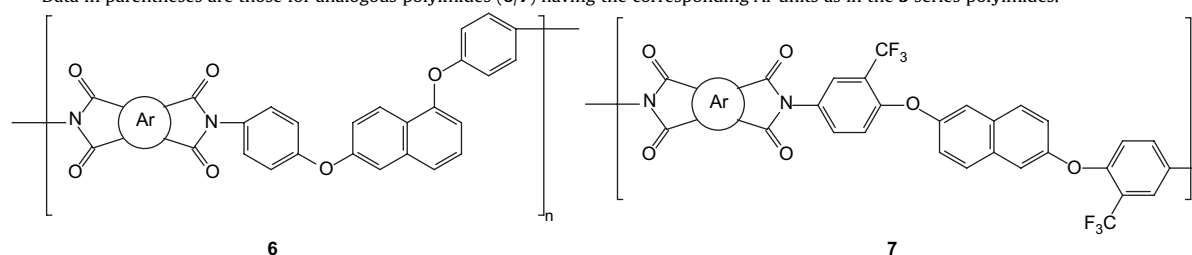


Table 4
Solubility behavior of the fluorinated polyimides prepared via chemical imidization^a

Solvent	Polyimide					
	5a	5b	5c	5d	5e	5f
NMP	+	+	+	+	+	+
DMAc	+h	+	+	+	+	+
DMF	+h	+h	+	+	+	+
DMSO	-	-	+	+	+	+
<i>m</i> -Cresol	-	+h	+h	+	+	+
2-Chlorophenol	+h	+	+	+	+	+
THF	-	-	+h	+	+	+
1,4-Dioxane	-	-	+h	+	+	+
Dichloromethane	-	-	+	+	+	+
Acetone	-	-	-	-	+	+

The symbol +: soluble at room temperature; +h: soluble on heating at 100 °C or boiling temperature; -: insoluble even on heating.

^a The solubility was determined by using 10 mg sample in 1 mL of stirred solvent.

The color intensities of the polyimides were elucidated from the yellowness (a^*) or redness (b^*) indices observed by a Macbeth color-eye colorimeter. The results shown in Table 5 indicate that the **5** series fluorinated polyimides generally showed a lower b^* value than the **6** series analogues without the CF_3 substituents. Moreover, thin films were measured for optical transparency using UV–vis spectroscopy, and the cutoff wavelengths (λ_0) from the UV–vis spectra are listed in Table 5. Consistent with the results obtained from colorimetry, all the fluorinated polyimides revealed a lower λ_0 than their respective CF_3 -free analogues. The films from fluorine-containing polyimides exhibited high percent transmittance values (>80%). The 6FDA and ODPAs produced fairly transparent and almost colorless polyimide films in contrast to other dianhydrides. These results were attributed to the reduction of the intermolecular charge-transfer complex (CTC) between alternating electron-donor (diamine) and electron-acceptor (dianhydride) moieties. The light colors of the polyimides with the CF_3 groups in their diamine moieties can be explained from the decreased intermolecular interactions. The bulky and electron-withdrawing CF_3 group in diamine **2** was effective in decreasing CTC formation between polymer chains through steric hindrance and the inductive effect (by decreasing the electron-donating property of diamine

Table 5

Color coordinates and cutoff wavelength (λ_o) from the UV–vis spectra of the polyimide films^a

Polymer	Film thickness (μm)	a^*	b^*	L^*	λ_o (nm)
Paper		-0.44	0.97	96.20	
5a	78	-4.24	70.25	87.24	428
5b	60	-1.17	44.21	86.36	412
5c	87	-6.76	35.65	85.05	427
5d	84	-1.17	21.20	90.45	378
5e	66	-8.07	34.29	89.70	408
5f	72	-4.05	13.36	94.28	376
6a	31	33.34	74.11	48.31	456
6b	47	20.76	53.17	58.39	427
6c	41	28.44	71.09	51.40	438
6d	34	16.83	40.66	65.42	392
6e	37	27.57	59.45	50.00	431
6f	38	25.35	47.35	60.41	400

^a The color parameters were calculated according to a CIE LAB equation, using paper as a standard. L^* is lightness; 100 means white, while 0 implies black. A positive a^* means red color, while a negative a^* indicates green color. A positive b^* means yellow color, while a negative b^* implies blue color.

moieties). A secondary positive effect of the CF_3 groups on the film transparency is the weakened intermolecular dispersion forces due to low polarizability of the C–F bond. The decrease in intermolecular CTC formation is understandable also from the significant solubility of the polyimides prepared from CF_3 -diamine **2**.

The thermal properties of the polyimides were determined by using DSC, TMA, and TGA (Table 6). DSC experiments were conducted at a heating rate of 20 °C/min in nitrogen. Rapid cooling from 400 °C to room temperature produced predominantly amorphous samples, so the T_g s of almost all the polyimides could be easily taken from the second DSC heating traces. The T_g values of the fluorinated polyimides ranged from 241 °C to 298 °C. The decreasing order of T_g generally correlates with that of the chain flexibility. Thus, the polyimide **5d** obtained from ODPDA showed the lowest T_g of 241 °C due to the presence of a flexible ether linkage between the phthalimide units, and the highest T_g of 298 °C was observed for polyimide **5a** derived from PMDA. Slightly lower T_g s for the **5a–5f** series in comparison with the **6a–6f** series might be a result of reduced interpolymer interaction and poor packing due to the bulky pendent CF_3 groups. In addition, the **5** series polyimides also exhibited a slightly lower T_g value compared to the **7** series counterpart because of the less symmetric structure of the

Table 6

Thermal behavior data of the polyimides

Polymer	T_g^a (°C)	T_s^b (°C)	T_d^c at 5 wt% loss (°C)		T_d at 10 wt% loss (°C)		Char yield ^d (%)
			In N_2	In air	In N_2	In air	
5a	298 (311) ^e	286	566	548	594	574	54
5b	266 (275)	253	562	544	588	572	61
5c	255 (256)	241	540	516	574	558	57
5d	241 (249)	231	552	532	582	563	58
5e	267 (275)	248	482	503	536	541	53
5f	260 (271)	242	532	519	553	538	51
6a	323	286	556	541	569	568	55
6b	264	248	572	560	592	581	66
6c	259	244	550	534	574	569	60
6d	249	227	559	537	574	572	58
6e	288	269	517	515	536	550	55
6f	276	261	533	520	554	543	58

^a Midpoint temperature of baseline shift on the second DSC heating trace (rate 20 °C/min) of the sample after quenching from 400 °C.

^b Softening temperature measured by TMA (penetration method) with a constant applied load of 10 mN at a heating rate of 10 °C/min. The film samples were heated at 300 °C for 30 min prior to the TMA experiments.

^c Decomposition temperatures recorded by TGA at a heating rate of 20 °C/min.

^d Residual weight percentage at 800 °C in nitrogen.

^e Data in parentheses are the reported values for the **7** series polyimides (see Ref. [40]).

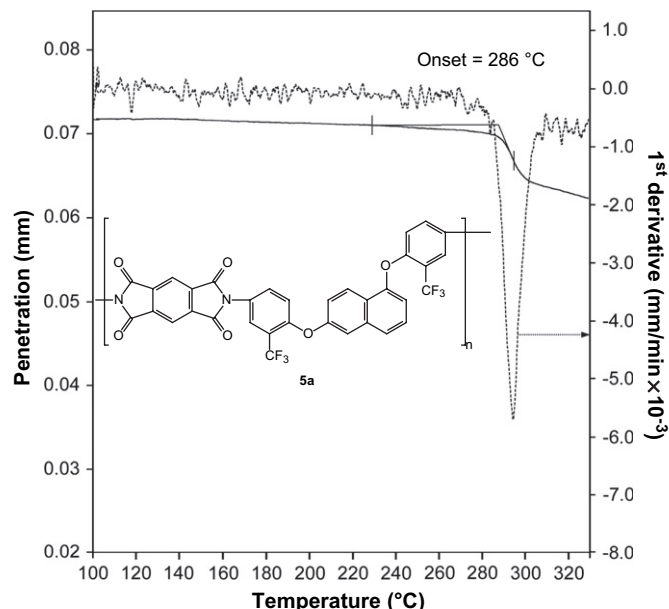


Fig. 6. Typical TMA thermogram of polyimide **5a** (heating rate = 10 °C/min; applied force = 10 mN).

diamine component. The softening temperatures (T_g) (may be referred as apparent T_g) of the polyimide films were determined by the TMA method using a loaded penetration probe. They were read from the onset temperature of the probe displacement on the TMA trace. As a representative example, the TMA trace of polyimide **5a** is illustrated in Fig. 6. The T_s values of the polyimides obtained by TMA are listed in Table 6. The trend of T_s variation with the chain stiffness is similar to that of T_g observed in the DSC measurements. The T_s values of the fluorinated polyimides (**5a–5f**) were lower than the T_g values by 10–18 °C. The relatively lower T_s values for these polyimides may indicate that they exhibit a higher degree of plasticity near T_g due to the increased free volume caused by the bulky CF_3 groups.

The thermal stability of the polyimides was evaluated by TGA measurements in both air and nitrogen atmospheres. Typical TGA curves for polyimides **5a** and **6a** are reproduced in Fig. 7. The decomposition temperatures (T_d s) at 5% and 10% weight loss in nitrogen and in air atmospheres were determined from the original TGA thermograms and are also given in Table 6. The T_d at 10% weight loss of the fluorinated polyimides (**5a–5f**) in nitrogen and air stayed in the range of 536–594 °C and 538–574 °C, respectively. They left more than 51% char yield at 800 °C in nitrogen. The TGA data indicated that these polyimides had fairly high thermal stability even with the introduction of bulky CF_3 pendent groups.

The dielectric constants and water absorption of all polyimides are presented in Table 7. In comparison, polyimides **5a–5f** revealed lower dielectric constants (2.75–3.13 at 10 kHz) than the corresponding homologous **6a–6f** polyimide films. Therefore, the 6FDA-derived polyimide **5f** exhibited the lowest dielectric constant of 2.75 at 10 kHz and water absorption due to the higher free volume and hydrophobicity. The low water absorptions ensure that these fluorinated polyimides have stable dielectric performance.

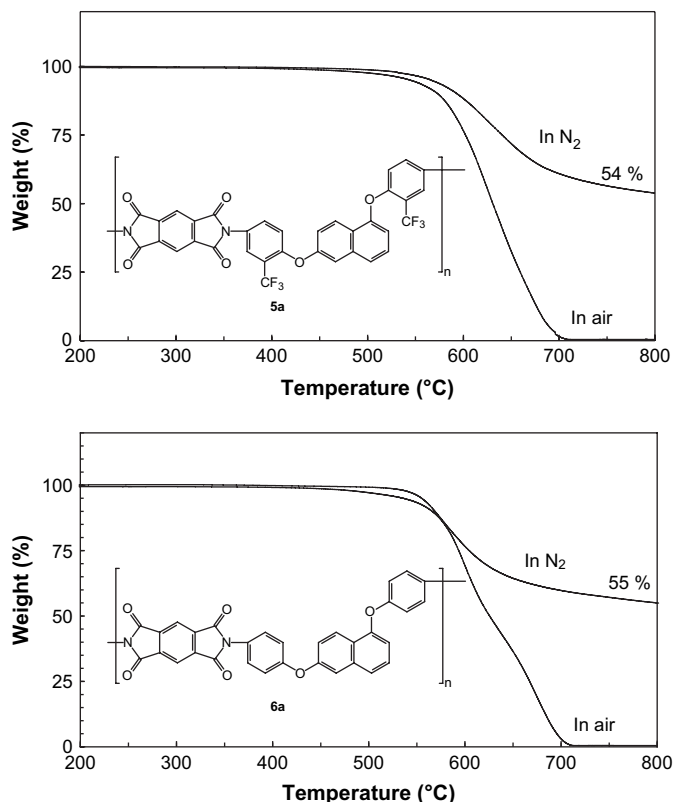


Fig. 7. TGA thermograms of polyimides **5a** and **6a** at a heating rate of 20 °C/min.

Table 7

Water absorption and dielectric constants of polyimides

Polymer code	Film thickness (μm)	Fluorine content (%)	Water absorption (%)	Dielectric constant (dry)	
				10 kHz	1 MHz
5a	78	17.6	0.52	2.94	2.89
5b	60	15.5	0.43	2.93	2.84
5c	87	14.9	0.44	3.13	3.07
5d	84	14.2	0.30	2.77	2.73
5e	66	15.2	0.26	3.12	3.00
5f	72	25.7	0.12	2.75	2.68
6a	31	0	0.84	3.02	3.00
6b	47	0	0.56	3.10	3.07
6c	41	0	0.69	3.22	3.19
6d	24	0	0.53	2.98	2.92
6e	37	0	0.78	3.31	3.28
6f	38	15.2	0.35	2.84	2.82

4. Conclusions

A novel fluorinated bis(ether amine) monomer, 1,6-bis(4-amino-2-trifluoromethylphenoxy)naphthalene, was prepared through the nucleophilic substitution reaction of 2-chloro-5-nitrobenzotrifluoride and 1,6-dihydroxynaphthalene, followed by hydrazine catalytic reduction of the dinitro intermediate. A series of organosoluble fluorinated polyimides have been synthesized from the trifluoromethyl-substituted bis(ether amine) with various aromatic dianhydrides by two-step thermal or chemical imidization method. The resulting polyimides could be cast into flexible and strong films with high solubility, high optical transparency, excellent thermal stability, moderate to high glass transition temperatures ($T_g = 241\text{--}298\text{ °C}$), and low dielectric constants. Thus, this series of polyimides exhibits a good combination of properties required for high-performance materials and demonstrates a promising potential for future application.

Acknowledgments

The authors are grateful to the National Science Council of the Republic of China for the financial support of this work.

References

- [1] Wilson D, Stenzenberger HD, Hergenrother PM, editors. Polyimides. London: Blackie; 1990.
- [2] Eastmond GC, Paprotny J. React Funct Polym 1996;30:27.
- [3] Eastmond GC, Paprotny J. Eur Polym J 1999;35:2097.
- [4] Imai Y. React Funct Polym 1996;30:3.
- [5] Hsiao S-H, Yang C-P, Chu K-Y. Macromolecules 1997;30:165.
- [6] Liou G-S, Maruyama M, Kakimoto M, Imai Y. J Polym Sci Part A Polym Chem 1998;36:2021.
- [7] Ayala D, Lozano AE, de Abajo J, de la Campa JG. J Polym Sci Part A Polym Chem 1999;37:805.
- [8] Li F, Ge JJ, Honigfort PS, Fang S, Chen J-C, Harris FW, et al. Polymer 1999;40:4987.
- [9] Yang C-P, Hsiao S-H, Yang H-W. Macromol Chem Phys 2000;20:409.
- [10] Myung BY, Kim JJ, Yoon TH. J Polym Sci Part A Polym Chem 2002;40:4217.
- [11] Hsiao S-H, Chung C-L, Lee M-L. J Polym Sci Part A Polym Chem 2004;42:1008.
- [12] Yang SY, Ge ZY, Yin DX, Liu JG, Li YF, Fan L. J Polym Sci Part A Polym Chem 2004;42:4143.
- [13] Zhang M, Wang Z, Gao LX, Ding MX. J Polym Sci Part A Polym Chem 2006;44:959.
- [14] Li WM, Li SH, Zhang QY, Zhang SB. Macromolecules 2007;40:8205.
- [15] Huang SJ, Hoyt AE. Trends Polym Sci 1995;3:262.
- [16] Tamai S, Yamaguchi A, Ohta M. Polymer 1996;37:3683.
- [17] Li F, Fang S, Ge JJ, Honigfort PS, Chen J-C, Harris FW, et al. Polymer 1999;40:4571.
- [18] de Abajo J, de la Campa JG. Adv Polym Sci 1999;140:23.
- [19] Jeong KU, Jo YJ, Yoon TH. J Polym Sci Part A Polym Chem 2001;39:3335.
- [20] Liu JG, Li ZX, Wu JT, Zhou HW, Wang FS, Yang SY. J Polym Sci Part A Polym Chem 2002;40:1583.
- [21] Reddy DS, Chou C-H, Shu C-F, Lee G-H. Polymer 2003;44:557.
- [22] Hsiao S-H, Huang T-L. J Polym Res 2004;1:9.
- [23] Hsiao S-H, Lin K-H. J Polym Sci Part A Polym Chem 2005;43:331.
- [24] Liaw D-J, Chang F-C, Leung M, Chou M-Y, Muellen K. Macromolecules 2005;38:4024.
- [25] Maier G. Prog Polym Sci 2001;26:3.
- [26] Chern Y-T, Shiue H-C. Macromolecules 1997;30:4646.
- [27] Chern Y-T, Shiue H-C. Macromol Chem Phys 1998;199:963.
- [28] Seino H, Mochizuki A, Ueda M. J Polym Sci Part A Polym Chem 1999;37:3584.
- [29] Watanabe Y, Shibasaki Y, Ando S, Ueda M. J Polym Sci Part A Polym Chem 2004;42:144.
- [30] Sasaki S, Nishi S. In: Ghosh MK, Mittal KL, editors. Polyimides: fundamentals and applications. New York: Marcel Dekker; 1996. p. 71–120 and references cited therein.
- [31] Hougham G. In: Hougham G, Cassidy PE, Johns K, Davidson T, editors. Fluoropolymers: synthesis and properties, vol. 2. New York: Kluwer Academic/Plenum; 1999. p. 233–76.
- [32] Ando S, Matsuura T, Sasaki S. In: Hougham G, Cassidy PE, Johns K, Davidson T, editors. Fluoropolymers: synthesis and properties, vol. 2. New York: Kluwer Academic/Plenum; 1999. p. 277–303.
- [33] Matsuura T, Ando S, Sasaki S. In: Hougham G, Cassidy PE, Johns K, Davidson T, editors. Fluoropolymers: synthesis and properties, vol. 2. New York: Kluwer Academic/Plenum; 1999. p. 305–50.
- [34] Harris FW, Li F, Cheng SZD. In: Hougham G, Cassidy PE, Johns K, Davidson T, editors. Fluoropolymers: synthesis and properties, vol. 2. New York: Kluwer Academic/Plenum; 1999. p. 351–70.
- [35] Hsiao S-H, Yang C-P, Chung C-L. J Polym Sci Part A Polym Chem 2003;41:2001.
- [36] Myung SY, Kim JS, Kim JJ, Yoon TH. J Polym Sci Part A Polym Chem 2003;41:3361.
- [37] Kute V, Banerjee S. Macromol Chem Phys 2003;204:2105.
- [38] Hsiao S-H, Chang Y-H. J Polym Sci Part A Polym Chem 2004;42:1255.
- [39] Yin DX, Li YF, Yang HX, Yang SY, Fan L, Liu JG. Polymer 2005;46:3119.
- [40] Yang C-P, Hsiao S-H, Chung C-L. Polym Int 2005;54:716.
- [41] Chung C-L, Tzu T-W, Hsiao S-H. J Polym Res 2006;13:495.
- [42] Shao Y, Li YF, Zhao X, Wang XL, Ma T, Yang FC. J Polym Sci Part A Polym Chem 2006;44:6836.
- [43] Liaw D-J, Huang C-C, Chen W-H. Macromol Chem Phys 2006;207:434.
- [44] Chen Y-Y, Yang C-P, Hsiao S-H. Macromol Chem Phys 2006;207:1888.
- [45] Yang C-P, Su Y-Y, Wen S-J, Hsiao S-H. Polymer 2006;47:7021.
- [46] Qiu Z, Wang J, Zhang Q, Zhang S, Ding M, Gao L. Polymer 2006;47:8444.
- [47] Jang WB, Shin DY, Choi SH, Park SG, Han HS. Polymer 2007;48:2130.
- [48] Yang C-P, Hsiao S-H, Jang C-C. J Polym Sci Part A Polym Chem 1995;33:1487.
- [49] Yang C-P, Hsiao S-H, Jang C-C. J Polym Sci Part A Polym Chem 1995;33:1095.